Journal of Computational Physics **152,** 736–755 (1999)
Article ID jcph.1999.6261, available online at http://www.idealibrary.com on IDEAL®

An Integral Computational Model for Crack Simulation and Detection via Eddy Currents

Raffaele Albanese,* Guglielmo Rubinacci,† and Fabio Villone†

*Associazione EURATOM/ENEA/CREATE, DIMET, Università degli Studi di Reggio Calabria, Via Graziella, Loc. Feo di Vito, I-89100, Reggio Calabria, Italy; †Associazione EURATOM/ENEA/CREATE, Dipartimento di Ingegneria Industriale, Università degli Studi di Cassino, Via Di Biasio 43, I-03043, Cassino (FR), Italy
E-mail: albanese@unirc.it, rubinacci@ing.unicas.it, villone@ing.unicas.it

Received August 3, 1998; revised February 24, 1999

In this paper an innovative technique is described to solve the electromagnetic problem in the presence of a cracked conductor. Both the direct problem (given the crack, compute the scattered field) and the inverse problem (given the external measurements, obtain the crack position and shape) are dealt with. The features of an integral formulation in terms of a two-component electric vector potential expanded over edge elements are fully exploited. The resulting method proves to be extremely efficient, also thanks to the binary nature of the unknown. In this paper we restrict our attention to a class of problems, namely the eddy current testing for thin cracks in non-magnetic metallic plates, but the method can be extended to more general cases. © 1999 Academic Press

Key Words: non-destructive evaluation; eddy currents; computational electromagnetics; finite elements; edge elements.

I. INTRODUCTION

Eddy current testing (ECT) is a non-destructive evaluation (NDE) technique that is gaining increasing interest as a key technology in the detection of small cracks in conductive specimen. Its main applications regard the analysis and testing of metallic components employed in transportation, nuclear, and other industrial plants [1]. The method is based on the detection of the magnetic field due to the eddy currents induced on the specimen. The presence of a defect modifies the eddy current pattern and hence gives rise to a field perturbation closely related to the position and shape of the defects. Thanks to a strong industrial concern, this kind of problem has been of considerable interest in the last years also from the computational viewpoint. This attention is well understood if one takes into account that fast and precise numerical methods are needed to post-process the magnetic

0021-9991/99 $30.00
Copyright © 1999 by Academic Press
All rights of reproduction in any form reserved.

measurements in order to attain an improved evaluation of the geometric characteristics of the flaw.

From the computational point of view, a direct and an inverse problem have to be solved. The direct problem consists of the evaluation of the field perturbation at the measurement probe locations, for a given exciting field and geometry of the flaw (or flaws). In the inverse problem, one has to find the position and the shape of the flaw(s), assuming the measurements and the forcing field as known quantities.

The inverse problem is non-linear and ill-posed. It is well known that a problem is well-posed in the sense of Hadamard if a solution exists, is unique, and depends continuously on the data. These aspects for the inverse electromagnetic problems have been studied by several authors. Here we just mention Colton and Kress [2], Colton and Paivarinta [3], Isakov [4], and Yamamoto [5]. Stability is usually achieved by means of suitable procedures like Tikhonov's regularization. Namely, a priori information about the solution is added and the problem is reformulated in order to restrict the set in which the solution is to be found. In the NDE, the problem is usually reformulated as the minimization of an error functional expressing the distance between computed and measured field values, with suitable assumptions about the solution (e.g., regularity, positiveness, topology of the support, etc.).

Solution of the inverse problem is the key objective in NDE. The success of any inversion procedure requires fast and accurate solutions of the forward problem. Basically, there are three main approaches to the numerical solution of this problem. The straightforward application of standard finite element techniques based either on differential or integral formulations [6], although easy to apply, often suffers from several drawbacks. In fact, the defect geometry and related field perturbations are very localized and impose severe constraints on the discretization of the specimen and, in some cases, of the region occupied by exciting sources and field sensors. A second approach is based on an integral formulation [7–10] specifically derived to deal with this kind of problem and numerically approximated by the method of moments. In this case, the unknowns are the equivalent sources consisting of volume current dipole distributions, usually approximated by piecewise constant vector pulse functions. In the integral equation, the dyadic Green's kernel already takes into account the correct continuity condition at the air/conductor interface, so that the discretized domain is limited to the flaw region. On the other hand, the need for an explicit knowledge of the Green's functions restricts the shape of the conductor to simple canonical geometries, such as a layered half space, an infinite cylinder, or a sphere [11,12].

Another formulation has been recently proposed and successfully applied [13–15] to keep the advantages of the integral approach without suffering from the restriction represented by the required knowledge of the analytic expression of Green's functions. The method is based on a differential formulation where the Green's function is numerically calculated using the solution of the field problem in the unflawed conducting domain.

The inverse problem related to the reconstruction of the geometric and physical characteristics of the defect requires, as already said, the minimization of an error functional related to the scattered field in the region outside the specimen. Strong difficulties arise since the possible presence of local minima requires global optimization procedures, such as simulating annealing or genetic algorithms that work efficiently only with a limited number of unknowns.

The problem of understanding the causes of the occurrence of local minima has been studied in [16], with reference to a quadratic expansion of the operator relating the scattered

field to the conductivity [17,18]. In the frame of this approach, a generalization of the well-known linear Born approximation, it has been shown that the presence of local minima is related to the ratio between the essential dimension of the subspace of data and the number of unknowns.

Deterministic methods used to find the solution of the inverse problem are usually based on gradient algorithms. In these cases, the gradient, or sensitivity, of the error functional with respect to the unknowns is often computed using the adjoint equation technique [19].

In summary, the main difficulties of the approaches mentioned above are the treatment of thin cracks, the need for a numerically consistent field representation (instead of pulse basis), time consuming forward solutions, unavailability of Green's functions, high discretization costs in the differential approaches, and the presence of a large number of unknowns in the inverse problem.

In this paper, to overcome these difficulties, we propose a numerical method for the reconstruction of thin cracks based on an efficient integral formulation in terms of a two-component current density vector potential [20] which takes advantage of the edge element representation of the field unknowns. Using superposition, the forward problem is reformulated as the determination of the modified eddy current pattern due to the presence of the defect. In particular, since the total current density has to be zero in the crack region, the variation of the current density is imposed to be just the opposite of the unperturbed one in the crack region, giving the known source term of an integral equation to be solved only around the crack. This fast algorithm to solve the forward problem is the key step of the inversion procedure. When generating the solution corresponding to a candidate flaw only a very small part of the whole matrix describing the model must be inverted.

The paper is organized as follows. Section II summarizes the main features of the integral formulation along with its discrete approximation. Sections III and IV discuss the proposed method, with reference to the direct and inverse problem, respectively. In Section V, the method is tested against some experimental results. In Section VI some final comments and conclusions are presented.

II. FORMULATION

The mathematical model consists of the set of the eddy current equations in linear non-magnetic media,

$$\nabla \times \mathbf{E} = -\partial \mathbf{B}/\partial t \qquad \text{in } V_c \tag{1}$$

$$\nabla \times \mathbf{H} = \mathbf{J} \qquad \text{in } V_c \tag{2}$$

$$\mathbf{B} = \mu_0 \mathbf{H} \qquad \text{in } V_c \tag{3}$$

$$\mathbf{J} = \sigma \mathbf{E} + \mathbf{J}_s \qquad \text{in } V_c, \tag{4}$$

where $\mathbf{E}$ is the electric field, $\mathbf{H}$ is the magnetic field, $\mathbf{B}$ is the magnetic flux density, $\mathbf{J}$ is the current density, $\mathbf{J}_s$ is the impressed current density, σ is the electrical conductivity, and μ_0 is the vacuum magnetic permeability.

Here, V_c is the conducting domain, i.e., the region of space where $\sigma \neq 0$, which will be supposed simply connected in the following to fix the ideas. Outside V_c, the following

equations hold:

$$\nabla \cdot \mathbf{B} = 0 \qquad \text{outside } V_c \tag{5}$$

$$\nabla \times \mathbf{H} = \mathbf{J}_s \qquad \text{outside } V_c \tag{6}$$

$$\mathbf{B} = \mu_0 \mathbf{H} \qquad \text{outside } V_c. \tag{7}$$

Of course, a suitable set of initial, boundary, and interface conditions must be imposed.

The formulation recalled here is presented in detail in [20, 21]. First of all, the following expression is used for the electric field, which automatically enforces Faraday's law,

$$\mathbf{E} = -\partial \mathbf{A}/\partial t - \nabla \varphi, \tag{8}$$

where φ is the electric scalar potential and $\mathbf{A}$ is the magnetic vector potential defined by Coulomb gauge,

$$\mathbf{B} = \nabla \times \mathbf{A}, \qquad \nabla \cdot \mathbf{A} = 0 \tag{9}$$

which can be linked to the unknown current density by

$$\mathbf{A}(\mathbf{x}, t) = \frac{\mu_0}{4\pi} \int_{V_c} \frac{\mathbf{J}(\mathbf{x}', t)}{|\mathbf{x} - \mathbf{x}'|} \, dV' + \mathbf{A}_s(\mathbf{x}, t), \tag{10}$$

where $\mathbf{A}_s$ is the vector potential due to the known source $\mathbf{J}_s$.

The second step is imposing Ohm's law using the weighted residual approach,

$$\int_{V_c} (\eta \mathbf{J} - \mathbf{E}) \cdot \mathbf{W} \, dV = 0, \qquad \mathbf{J} \in S, \forall \mathbf{W} \in S, \tag{11}$$

where $\eta = 1/\sigma$ is the electric resistivity, $S = \{\mathbf{J} \in \mathbf{L}^2{}_{\text{div}}(V_c), \boldsymbol{\nabla} \cdot \mathbf{J} = 0 \text{ in } V_c, \mathbf{J} \cdot \mathbf{n} = 0 \text{ on } \partial V_c\}$, and $\mathbf{L}^2{}_{\text{div}}(V_c)$ is the space of vector fields that are square integrable in V_c together with their divergence. Note that the condition $\mathbf{J} \in S$, which implies the continuity of the normal component of $\mathbf{J}$, comes from (2) and the continuity of the tangential components of $\mathbf{H}$. On the contrary, the condition that also the weighting function $\mathbf{W} \in S$ is a numerical choice, which allows us to remove the contribution of the electric scalar potential in (11), that becomes

$$\int_{V_c} \mathbf{W} \cdot \left(\eta \mathbf{J} - \frac{\partial}{\partial t} \left(\frac{\mu_0}{4\pi} \int_{V_c} \frac{\mathbf{J}(\mathbf{x}', t)}{|\mathbf{x} - \mathbf{x}'|} \, dV' + \mathbf{A}_s(\mathbf{x}, t) \right) \right) dV, \qquad \mathbf{J} \in S, \forall \mathbf{W} \in S. \tag{12}$$

As a consequence, the electric scalar potential disappears from the formulation, and no potential jump must be considered on ∂V_c.

The next step is the numerical solution of (12). A discretization of the conducting domain is given in terms of a finite element mesh. The condition $\mathbf{J} \in S$ is imposed expanding $\mathbf{J} = \sum_k I_k \mathbf{J}_k$ on a set of basis functions $\mathbf{J}_k$ which in turn belong to S. This is guaranteed by introducing the electric vector potential $\mathbf{T}$, such that $\nabla \times \mathbf{T} = \mathbf{J}$, and expanding it on an edge element basis $\mathbf{N}_j$, as $\mathbf{T} = \sum_j I_j \mathbf{N}_j$ [21]. Doing so, the coefficient I_j is the line integral of $\mathbf{T}$ along the edge j. The uniqueness of $\mathbf{T}$ is guaranteed by means of the two-component gauge [22, 21],

$$\mathbf{T} \cdot \mathbf{w} = 0, \tag{13}$$

where $\mathbf{w}$ is an arbitrary vector field with no closed field lines. The imposition of this gauge is very conveniently implemented using a tree–cotree decomposition of the graph G made of the nodes N and the edges E of the mesh [20, 21]. The vector field $\mathbf{w}$ is chosen such that its field lines are along the branches of a tree T, which does not close any loop by definition. Hence, the coefficients I_j linked to all the branches of the tree vanish, and only the coefficients related to the edges of the cotree $\mathsf{C} = \mathsf{G} - \mathsf{T}$ are retained. Any of these coefficients, say I_k, is then the current flux linked by the loop closed by the edge k of the cotree with the branches of the tree.

It is also straightforward to enforce the additional condition required to the functions of S:

$$\mathbf{J} \cdot \mathbf{n} = 0 \qquad \text{on } \partial V_c. \tag{14}$$

Let G_b be the subgraph of G including only boundary nodes (N_b) and edges (E_b). Using a sequential algorithm, it is always possible to select T so that $\mathsf{T} \cap \mathsf{E}_b$ is a tree for G_b [20]. With such a choice, for a simply connected region, all the cotree edges on the boundary ($\mathsf{C} \cap \mathsf{E}_b$) close loops completely laying on ∂V_c, and therefore the corresponding coefficients must vanish.

As a consequence, the basis functions $\mathbf{J}_k = \nabla \times \mathbf{N}_k$ of the current density automatically belong to S, and so does $\mathbf{J}$. The degrees of freedom I_k of the expansion

$$\mathbf{J} = \sum_k I_k \nabla \times \mathbf{N}_k \tag{15}$$

have the following property. Given a mesh facet f, let $k_1, \ldots, k_r$ be the indices of the active (i.e., non-vanishing) edges which are part of the contour ∂f of f. Then, the current flux through f is simply

$$G_f = \pm I_{k1} \pm \cdots \pm I_{kr}, \tag{16}$$

where the signs depend on the relative orientation of the edges and ∂f.

Adopting the Galerkin method, i.e., choosing the $\mathbf{W}$'s equal to the basis functions $\mathbf{J}_k$'s, Eq. (12) can be written as

$$\mathsf{L}\frac{d\mathbf{I}}{dt} + \mathsf{R}\mathbf{I} = \mathbf{V}, \tag{17}$$

where $\mathbf{I} = \{I_k\}$, $\mathbf{V} = \{V_k\}$, and

$$L_{ij} = \frac{\mu_0}{4\pi} \int_{V_c} \int_{V_c} \frac{\nabla \times \mathbf{N}_i(\mathbf{x}) \cdot \nabla \times \mathbf{N}_i(\mathbf{x}')}{|\mathbf{x} - \mathbf{x}'|} \, dV \, dV' \tag{18}$$

$$R_{ij} = \int_{V_c} \nabla \times \mathbf{N}_i(\mathbf{x}) \cdot \eta \nabla \times \mathbf{N}_j(\mathbf{x}) \, dV \tag{19}$$

$$V_i = -\frac{\partial}{\partial t} \int_{V_c} \nabla \times \mathbf{N}_i(\mathbf{x}) \cdot \mathbf{A}_s(\mathbf{x}) \, dV. \tag{20}$$

Of course, if a sinusoidal steady state must be studied (which is common practice in electromagnetic non-destructive evaluation), the impedance $\mathbf{Z} = (\mathbf{R} + j\omega\mathbf{L})$ can be introduced,

$$(\mathbf{R} + j\omega\mathbf{L})\mathbf{I} = \mathbf{V}, \tag{21}$$

where the elements of $\mathbf{I}$ and $\mathbf{V}$ are phasors.

III. SOLUTION OF THE DIRECT PROBLEM

Simplifying Assumptions

As mentioned above, we restrict our attention to a class of problems, namely the eddy current testing for thin cracks in non-magnetic metallic plates.

The first assumption is that the thickness of the defect is small when compared not only to its depth and width but also to the skin depth at the exciting frequency. This allows us to schematize the defect as a zero-thickness crack, i.e., as a surface across which the current flow is forbidden. Anyway, the present method can be easily extended to the case of volumetric flaws.

The absence of non-linear media allows us not only to use the integral formulation described in Section II but also to exploit superposition and reciprocity to improve the accuracy of the numerical results for a given computation effort.

Solution of the Flawless Problem

First, we calculate the solution of the electromagnetic problem without the flaw. Analytical solutions are available for particular forms of the conducting structures, e.g., for an indefinite plate [23]. These analytical solutions provide acceptable approximations in most practical cases.

Otherwise, if the edge effects are not negligible, or the shape of the specimen is not canonical, the unperturbed field can be determined numerically by means of the technique illustrated in Section II. Expanding the current density as $\mathbf{J}_0 = \sum I_{0k}\mathbf{J}_{0k}$, Eq. (21) yields

$$\mathbf{Z}_0\mathbf{I}_0 = \mathbf{V}_0, \tag{22}$$

where $\mathbf{Z}_0 = \mathbf{R}_0 + j\omega\mathbf{L}_0$ is the impedance matrix, and $\mathbf{V}_0$ is the applied voltage. The subscript 0 indicates that the shape functions, the matrices, and the solution coefficients are calculated in the absence of the crack.

Calculation of the Modified Eddy Current Pattern

The second step for the solution of the forward problem is the determination of the modified eddy current pattern due to the presence of the defect. A thin crack can be described as a surface Σ_d, discretized via a set of finite element faces characterized by the constraint

$$\mathbf{J} \cdot \mathbf{n} = 0, \tag{23}$$

where $\mathbf{n}$ is the normal unit vector on the face.

To solve a single problem in the presence of a well defined flaw, it is possible to treat $\partial V_c \cup \Sigma_d$ with the technique described in Section II to deal with condition (14). However, it is often required to solve the direct problem several times for the same specimen with different defects, e.g., when solving the inverse problem. In this case the above technique is not efficient at all, because the change of Σ_d implies redefinition of the tree and reassembling of the matrices. For this reason we adopt the following method.

The flux of $\mathbf{J} = \nabla \times \mathbf{T}$ across any elementary face is given by the circulation of $\mathbf{T}$ along the edges identifying the face. As the values of the unknowns I_k's represent the line integrals

of $\mathbf{T}$ along the active edges, the net current crossing an elementary face is given by the algebraic sum of the unknowns associated with the active edges of the face [24],

$$\mathbf{G} = \mathbf{P}\mathbf{I}, \tag{24}$$

where $\mathbf{G}$ is the set of net currents crossing the m facets of Σ_d, and $\mathbf{P}$ is a (m, n) sub-matrix of the edge-facet incidence matrix with coefficients 0, $+1$, or -1.

In principle, the desired result might be obtained by calculating the eddy current density induced by the exciting coil in the presence of the crack, obtaining the corresponding signal, and subtracting the signal obtained without the flaw. However, to avoid cancellation errors, we exploit superposition, assuming directly the variation $\delta\mathbf{J}$ of the eddy current density as unknown,

$$\mathbf{J} = \mathbf{J}_0 + \delta\mathbf{J}. \tag{25}$$

We also expand $\delta\mathbf{J}$ in terms of the solenoidal shape functions used for the flawless plate:

$$\delta\mathbf{J} = \sum_{k=1,n} \delta I_k \mathbf{J}_{0k}. \tag{26}$$

However, to satisfy Eq. (23), the variation of the normal component of the current density must be just the opposite of the unperturbed one across the crack. We therefore impose the constraint

$$\mathbf{P}\delta\mathbf{I} = -\mathbf{G}_0, \tag{27}$$

where

$$\mathbf{G}_0 = \mathbf{P}\mathbf{I}_0 \tag{28}$$

is the set of unperturbed currents crossing the crack facets.

In this case, the unknown can be expressed as

$$\delta\mathbf{I} = \mathbf{K}\delta\mathbf{X} + \delta\mathbf{I}_p, \tag{29}$$

where $\mathbf{K}$ is a $(n, n - m)$ matrix given by an orthonormal basis for the null space of $\mathbf{P}$, $\delta\mathbf{I}_p$ is an arbitrary solution of Eq. (27), and $\delta\mathbf{X}$ is an auxiliary variable.

A possible choice for $\delta\mathbf{I}_p$ is provided by pseudo-inversion of system (27),

$$\delta\mathbf{I}_p = \mathbf{S}\delta\mathbf{G}, \tag{30}$$

where $\delta\mathbf{G} = -\mathbf{G}_0$ and $\mathbf{S} = \mathbf{P}^+$. In this way Eq. (29) becomes

$$\delta\mathbf{I} = \mathbf{K}\delta\mathbf{X} + \mathbf{S}\delta\mathbf{G}. \tag{31}$$

This allows us to express $\delta\mathbf{I}$ in terms of the $n - m$ unknown vector $\delta\mathbf{X}$ and the m known vector $\delta\mathbf{G} = -\mathbf{G}_0$. Hence, the problem becomes finding $\delta\mathbf{X}$. However, we cannot use Eq. (12) with the n $\mathbf{J}_{0i}$'s as weighting functions, unless we explicitly introduce the jump of the scalar potential across the crack, since they do not fulfill constraint (23). A more efficient

alternative is to consider a set of weighting functions satisfying Eq. (23) across the crack. These are readily obtained observing that $\mathbf{PK}\delta\mathbf{X} = 0$ for any $\delta\mathbf{X}$. As a consequence, a set of independent weighting functions is given by the linear combinations of J_{0k}'s with the coefficients of the columns of $\mathbf{K}$, i.e., the $n-m$ rows of $\mathbf{K}^{\mathrm{T}}$. The corresponding linear system for the calculation of $\delta\mathbf{J}$ is therefore

$$\mathbf{K}^{\mathrm{T}}\mathbf{Z}\mathbf{K}\delta\mathbf{X} = -\mathbf{K}^{\mathrm{T}}\mathbf{Z}\mathbf{S}\delta\mathbf{G}. \tag{32}$$

The eddy current perturbation is finally $\delta\mathbf{J} = \sum_{k=1,n}\delta I_k\mathbf{J}_{0k}$, where $\delta\mathbf{X}$ is calculated from Eq. (32) and $\delta\mathbf{I}$ is obtained from (31).

Calculation of the Perturbed Signals

From the eddy current perturbation $\delta\mathbf{J} = \sum\delta I_k\nabla\times\mathbf{N}_{\mathrm{k}}$ we may compute the reaction field. In particular, the impedance change of the exciting coil is given by any of the expressions

$$\delta Z = j\omega\int_{Ds}\delta\mathbf{A}\cdot\mathbf{J}_{\mathrm{s}}\,dV/I_s^2 \tag{33}$$

$$\delta Z = j\omega\int_{Dc}\mathbf{A}_{\mathrm{s}}\cdot\delta\mathbf{J}\,dV/I_s^2 \tag{34}$$

$$\delta Z = -\mathbf{V}_0^{\mathrm{T}}\delta\mathbf{I}/I_s^2, \tag{35}$$

where $\delta\mathbf{A}$ is the magnetic vector potential due to $\delta\mathbf{J}$.

Equation (33) is the standard expression, whereas Eqs. (34) and (35), which generally yield more accurate results, are obtained using reciprocity. Equation (35) can be used if the unperturbed problem has been solved numerically.

IV. SOLUTION OF THE INVERSE PROBLEM

When solving the direct problem the position of the crack is known *a priori*. Hence, the $\mathbf{P}$ matrix is constructed only on the mesh facets which belong to the crack itself, and only the equations regarding $\delta\mathbf{X}$ must be written, since $\delta\mathbf{G}$ is equal to the opposite of the unperturbed current flux vector $-\mathbf{G}_0$.

Conversely, the inverse problem consists of finding the unknown position and shape of the crack from the knowledge of some external measurements. From our point of view, we must find which is the set of mesh facets belonging to the crack. As a consequence, for each facet of the mesh we must understand whether it is part of the crack or not. It is worth noticing that the problem involves a binary decision: once we have ascertained that a facet indeed belongs to the crack the value of the current flowing through it is known, since it must be the opposite of the unperturbed current. On the contrary, if the facet is not part of the flaw, the value of current flow is unknown. Of course, such a "bitmap" description of the crack is expected to get more and more accurate as the discretization gets finer.

Moreover, we will assume that it is possible, from the external electromagnetic measurements, to gain rough information about the zone of the specimen where the crack is presumably located. Once this has been attained, one may perform a higher number of measurements only close to this region. In this way, the inverse problem that we tackle

is

find the position and shape of the crack starting from some electromagnetic external measurements and some a priori rough information about the region where the crack is presumably located.

This method is a common practice in standard eddy current non-destructive evaluation [25, 26].

Finally, some considerations are called for about the fact that the problem is ill-posed. As mentioned in the Introduction, the solution of the inverse problem needs regularization by restricting the set in which we look for the solution. In our approach the regularization acts at the following levels.

(a) The unknown is binary, i.e., for each facet of the mesh we must decide whether it belongs to the crack or not. This feature of the method eliminates all the possible solutions corresponding to intermediate situations in which the facet can be partially crossed by currents.

(b) We have identified the zone where the crack is located. This means that we are disregarding all the spurious solutions corresponding to non-physical cracks located in a region where we know a priori that no defects are present.

(c) Further steps in this direction of reducing the space of the unknown may be done for each single problem. For instance it may be possible to assume that the defect is superficial and simply connected. In Section V we will give some further hints, when presenting the results of the inverse problem.

From the above considerations the following strategy comes out for the solution of the inverse problem. First of all, we identify the set T of all possible candidate crack facets, i.e., the set of all mesh facets which could possibly belong to the crack. Then, we calculate $\mathbf{G}_0$ and the $\mathbf{P}$ matrix on this set and we perform the variable change just as in the case of the direct problem. However, now not all the $\delta\mathbf{G}$ are known, since only some of them will belong to the crack. Hence, the inverse problem can be reformulated as

find the subset $B \subseteq T$ such that the solution obtained imposing $\delta\mathbf{G}_B = -\mathbf{G}_{0B}$ gives the best fit to the experimental data,

where $\delta\mathbf{G}_B$ ($\mathbf{G}_{0B}$) are the current fluxes (unperturbed current fluxes) through the mesh facets belonging to B.

Because of the particular nature of this problem, a binary optimization technique seems to be particularly suitable. Indeed, what must be found is the bit string codifying which facets of T belong to B. Examples of such methods are the genetic algorithms. The key to these techniques is making successive tentative choices for the subset B, refining at each step.

Hence, a fast method for solving the direct problem corresponding to each tentative choice must be available. Now, we discuss the method for solving the problem once the subset B has been chosen on the basis of the optimization strategy.

Let $F = T - B$ be the set of facets belonging to the tentative set T but not to the crack B. The corresponding current fluxes $\delta\mathbf{G}_F$ are not known *a priori*, and hence the relative equations must be imposed, together with the equations corresponding to $\delta\mathbf{X}$, which are unknown, as in the direct problem.

In other words, first of all we define

$$\mathbf{Z}_{XX} = \mathbf{K}^{\mathrm{T}}\mathbf{Z}\mathbf{K}; \qquad \mathbf{Z}_{XG} = \mathbf{Z}_{GX}^{\mathrm{T}} = \mathbf{K}^{\mathrm{T}}\mathbf{Z}\mathbf{S}; \qquad \mathbf{Z}_{GG} = \mathbf{S}^{\mathrm{T}}\mathbf{Z}\mathbf{S}. \tag{36}$$

Then, we say that by substituting the subscript G with B or F we obtain the submatrix resulting from considering only the rows or the columns relative to the facets belonging to B and F, respectively: for instance, $\mathbf{Z}_{XF}$ is the submatrix of $\mathbf{Z}_{XG}$ obtained by selecting the columns corresponding to facets belonging to F.

Finally, we can write

$$\mathbf{Z}_{XX}\delta\mathbf{X} + \mathbf{Z}_{XF}\delta\mathbf{G}_F + \mathbf{Z}_{XB}\delta\mathbf{G}_B = 0 \tag{37}$$

$$\mathbf{Z}_{FX}\delta\mathbf{X} + \mathbf{Z}_{FF}\delta\mathbf{G}_F + \mathbf{Z}_{FB}\delta\mathbf{G}_B = 0, \tag{38}$$

where

$$\delta\mathbf{G}_B = -\mathbf{G}_{0B}. \tag{39}$$

System (37)–(38) must be solved in order to obtain the unknowns $\delta\mathbf{X}$ and $\delta\mathbf{G}_F$ for a given subset B.

Obtaining $\delta\mathbf{X}$ from (37)

$$\delta\boldsymbol{X} = -(\mathbf{Z}_{XX})^{-1}\mathbf{Z}_{XG}\delta\mathbf{G} = -(\mathbf{Z}_{XX})^{-1}(\mathbf{Z}_{XF}\delta\mathbf{G}_F + \mathbf{Z}_{XB}\delta\mathbf{G}_B) \tag{40}$$

and substituting in (38), taking account of (39), we obtain

$$\mathbf{Z}'_{FF}\delta\mathbf{G}_F = \mathbf{Z}'_{FB}\mathbf{G}_{0B}, \tag{41}$$

where $\mathbf{Z}'_{FF} = \mathbf{Z}_{FX}(\mathbf{Z}_{XX})^{-1}\mathbf{Z}_{XF} - \mathbf{Z}_{FF}$ and $\mathbf{Z}'_{FB} = \mathbf{Z}_{FX}(\mathbf{Z}_{XX})^{-1}\mathbf{Z}_{XB} - \mathbf{Z}_{FB}$.

Hence, we can find $(\mathbf{Z}_{XX})^{-1}\mathbf{Z}_{XG}$ and $\mathbf{Z}'_{GG} = \mathbf{Z}_{GX}(\mathbf{Z}_{XX})^{-1}\mathbf{Z}_{XG} - \mathbf{Z}_{GG}$ once and for all; $\mathbf{Z}'_{FF}$ and $\mathbf{Z}'_{FB}$ are suitable submatrices of $\mathbf{Z}'_{GG}$. Then, only the matrix $\mathbf{Z}'_{FF}$ must be inverted at each step in order to find $\delta\mathbf{G}_F$, and only a matrix-by-vector product is needed for $\delta\mathbf{X}$. Once $\delta\mathbf{X}$ and $\delta\mathbf{G}$ are known, it is possible to get the original unknowns $\delta\mathbf{I}$ from (31) and in turn any other possible output variable (field measurements, impedance variation, etc.).

If we know roughly which is the zone of the specimen where the crack is located, then the number n_T of facets belonging to T will be much smaller than the total number of unknowns, and hence the inversion of $\mathbf{Z}'_{FF}$ (which is $(n_T - n_B) \times (n_T - n_B)$, where n_B is the number of facets in B) is not computationally very heavy. A further speed-up is obtained by applying Woodbury's algorithm [27], briefly recalled in the Appendix. Indeed, using this algorithm it is possible to solve the problem just inverting a matrix of dimensions n_B. Hence, for each choice of the subset B the dimension of the matrix to be inverted is $\min(n_T - n_B, n_B)$, which is at most $n_{\max} = n_T/2$. Alternative applications of Woodbury's algorithm can also be made throughout the iteration process for the solution of the inverse problem, when knowing the inverse of a number of submatrices of $\mathbf{Z}'_{GG}$.

If the impedance variation is sought, a further simplification is possible. Indeed, from (35) we have

$$-\delta Z I_s^2 = \mathbf{V}_0^{\mathrm{T}}\delta\mathbf{I} = \mathbf{V}_{N0}^{\mathrm{T}}\delta\mathbf{Y}, \tag{42}$$

where $\mathbf{V}_{N0} = \mathbf{H}^{\mathrm{T}}\mathbf{V}_0$ and, as usual, $\delta\mathbf{I} = \mathbf{H}\delta\mathbf{Y}$ with $\mathbf{H} = [\mathbf{K}\,\mathbf{S}]$, $\delta\mathbf{Y} = [\delta\mathbf{X};\,\delta\mathbf{G}]$. It results that

$$\mathbf{Z}_N\mathbf{Y}_0 = \mathbf{V}_{N0}, \tag{43}$$

where $\mathbf{Z}_N = \begin{bmatrix} \mathbf{Z}_{XX} & \mathbf{Z}_{XG} \\ \mathbf{Z}_{GX} & \mathbf{Z}_{GG} \end{bmatrix}$ and $\mathbf{Y}_0 = \begin{bmatrix} \mathbf{X}_0 \\ \mathbf{G}_0 \end{bmatrix}$ is the unperturbed solution in terms of the new variables. Hence, from (42) we have

$$-\delta Z I_s^2 = \mathbf{Y}_0^{\mathrm{T}} \mathbf{Z}_N \delta \mathbf{Y} = \mathbf{X}_0^{\mathrm{T}} (\mathbf{Z}_{XX} \delta \mathbf{X} + \mathbf{Z}_{XG} \delta \mathbf{G}) + \mathbf{G}_0^{\mathrm{T}} (\mathbf{Z}_{GX} \delta \mathbf{X} + \mathbf{Z}_{GG} \delta \mathbf{G}). \tag{44}$$

Using (40) we finally obtain

$$\delta Z I_s^2 = \mathbf{G}_0^{\mathrm{T}} \mathbf{Z}'_{GG} \delta \mathbf{G}, \tag{45}$$

where $\mathbf{G}_0$ is the vector of unperturbed current fluxes through *all* the tentative facets in T; $\delta \mathbf{G}$ is the vector of the actual current fluxes through all the tentative facets in T, so that it will be made of $\delta \mathbf{G}_B = -\mathbf{G}_{0B}$ and $\delta \mathbf{G}_F$ which must be found solving (41). In other words, if the impedance variation is sought, only the matrix $\mathbf{Z}'_{GG}$ is needed both for inversion and for multiplication.

V. EXAMPLES OF APPLICATION

In this section we present some examples of application of the method to both the direct and the inverse problem. The configuration is the JSAEM Problem 6 [1]: a pancake type probe coil (internal radius 0.6 mm, external radius 1.6 mm, height 0.8 mm, lift off 0.5 mm) is placed above a finite plate of dimensions 140 × 140 × 1.25 mm, having a resistivity of 10^{-6} Ωm.

Direct Problem

The direct problem consists of the determination of the impedance change of the pancake coil due to the presence of a small thin crack (10 mm long), of four different shapes (see Fig. 1), elliptical, sloping, stepwise, and rectangular, both on the same side of the plate as

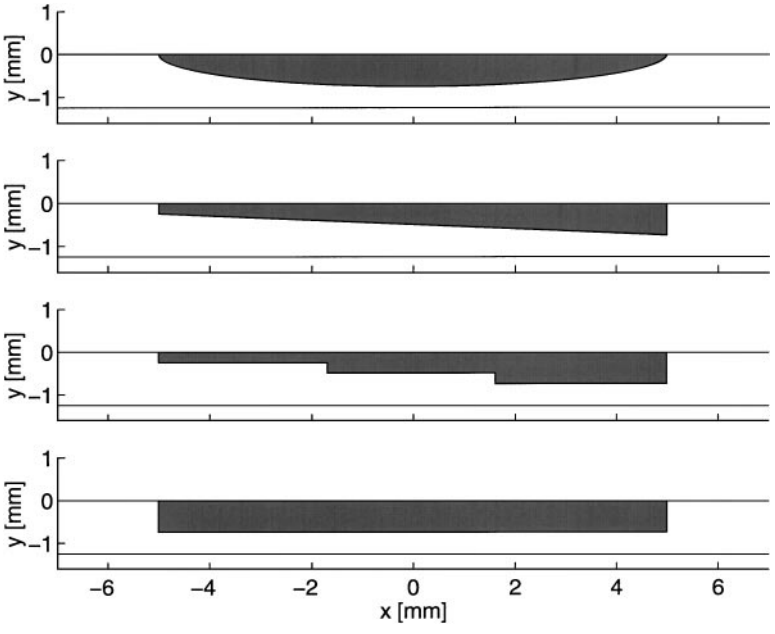

FIG. 1. Different crack shapes for JSAEM Benchmark Problem 6.

TABLE I
Mesh Details for the Meshes Used at Both Frequencies

Nodes	Elements	Edges	Active edges
1200	840	3202	1477

the coil (inner defect) or on the other side (outer defect). The width of the defect ranges from 0.22 to 0.25 mm for the different shapes. The excitation frequencies are 150 and 300 KHz, and the allowed coil positions cover the range $-10 < x < 10$ mm, $y = 0$ (the crack is in the $y = 0$ plane, centered around $x = 0$).

First of all, we must discuss the validity of the thin crack approximation. The width of the crack is much smaller than the other dimensions, which is the first obvious condition that must be satisfied. In addition, this width must be much smaller than the penetration depth. Indeed, if this were not the case, the length of the current paths originating from the crack in order to compensate for the unperturbed current would be comparable with the crack width. This clearly invalidates the assumption of a thin crack. The penetration depths are 1.30 and 0.92 mm for the two frequencies; hence, the thin crack approximation can be assumed as valid, since the width is more than 4 times smaller than the penetration depth.

The first thing to do is to give a finite element mesh of the domain of interest. Since we are solving for the perturbation of the current pattern we only need to discretize the region immediately around the crack itself, possibly truncating the real domain. Indeed, the only thing that must be verified is that the perturbation current pattern is not affected by the fictitious boundaries, regardless of the position of the excitation.

Because of the different penetration depths in the two cases, we used two different meshes: the discretized regions are $25 \times 16 \times 1.25$ mm and $25 \times 11 \times 1.25$ mm in the two cases, respectively, but the topological properties (summarized in Table I) are the same (see also Fig. 2). The discretized zone has been reduced in the y direction in the high frequency case because the current perturbation is closer to the crack because of the reduced penetration depth. In both cases we exploited the symmetry with respect to the y direction, imposing the perturbed current density to be purely normal to the plane $y = 0$. On the other hand we did not exploit the symmetry condition at $x = 0$. The mesh does not follow the known profile of the crack, but is just made of regular hexahedral elements. Hence, the crack will be approximated as a combination of rectangular facets.

Once the mesh has been given, the complex matrix $\mathbf{Z}$ is constructed. Then, the matrix $\mathbf{P}$ is calculated, together with its pseudoinverse $\mathbf{S}$ and its null $\mathbf{K}$; finally, the matrix $\mathbf{Z}'_{GG}$ is computed once and for all. The latter is the only thing needed, since only the impedance variation is sought. Of course, these calculations must be performed on the two different mesh configurations corresponding to the two frequencies.

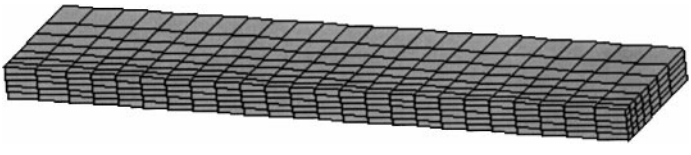

FIG. 2. The 3-D view of the mesh.

The geometry of the excitation is taken into account only in the solution of the unperturbed problem. Since the plate is large enough with respect to the coil and the crack to disregard any edge effect, we use the analytical solution described in [23] for the solution of the unperturbed problem in terms of current density. Then, this current density is numerically integrated on the various mesh facets belonging to the crack, which gives the $\mathbf{G}_0$ vector mentioned before. We explicitly notice that this is not a limitation of the method; if an analytical solution had not been available a numerical solution could be used as well, without any modifications of the procedure. In this case, a larger mesh should have been used, since generally speaking a fictitious boundary that does not affect the perturbation may well have a strong influence on the current induced by the excitation. This additional mesh would have been used only for the solution of the unperturbed problem, playing no further role in the solution either of the direct or the inverse problem. This means that the possible additional computational costs can be paid once and for all.

In Figs. 3 and 4 the results are presented for the direct problem, in the case of the rectangular inner defect at 300 KHz and of the elliptical outer defect at 150 KHz. The crack configuration is schematized as a set of rectangular (gray) facets. This discretization exactly fits the crack shape in the rectangular case; for the elliptical configuration a stepwise approximation is used. The impedance variation is plotted in the two cases for each position of the coil.

The predictions are satisfactory in both cases, not only qualitatively but also quantitatively. Where the agreement is poor, the difference seems to be due more to the error bars of the measurement than to the discretization error of the numerical solution. Indeed, where the prediction does not fit the data usually the measurements are not symmetric with respect to the $x = 0$ plane, whereas the crack configurations (and the predictions) are symmetric.

Inverse Problem

Now we tackle the inverse problem: given the experimental impedance variations as described before, and some rough information about the crack location, the crack position and shape must be identified. Of course, all the difficulties briefly recalled in the Introduction related to the ill-posedness and non-linearity of the problem must be kept in mind when solving it. Anyway, here we mainly focus on the features of the method of solution rather than on the basic mathematical aspects of the question.

The first thing to do is to choose the set T of candidate mesh facets which can possibly belong to the crack. We suppose that T is made by all the facets belonging to the $y = 0$ plane of the mesh, apart from the extreme ones; the total number of facets belonging to T is $n_T = 100$. We then calculate the $\mathbf{Z}'_{GG}$ matrix for this set of facets once and for all.

The optimization procedure used in this paper in order to find the optimal subset B of T falls in the stream of genetic algorithms. We assume as unknown the string made of the depth of the crack at each column of the mesh; hence, for instance, the string [1 3 0 2 4 3 5 0 2 5 4 1 0 2 2 3 4 5 1 2] represents the crack shown in Fig. 5. This means that we are assuming to know a priori that the crack is superficial; this is not a limitation of the method, which can easily deal with buried cracks and unconnected cracks, but only a further regularization adopted in order to solve the inverse problem [25].

Starting from an initial random set of strings, the population is evolved using the classical rules of genetic algorithms: crossover and mutation [28]. The various strings are classified

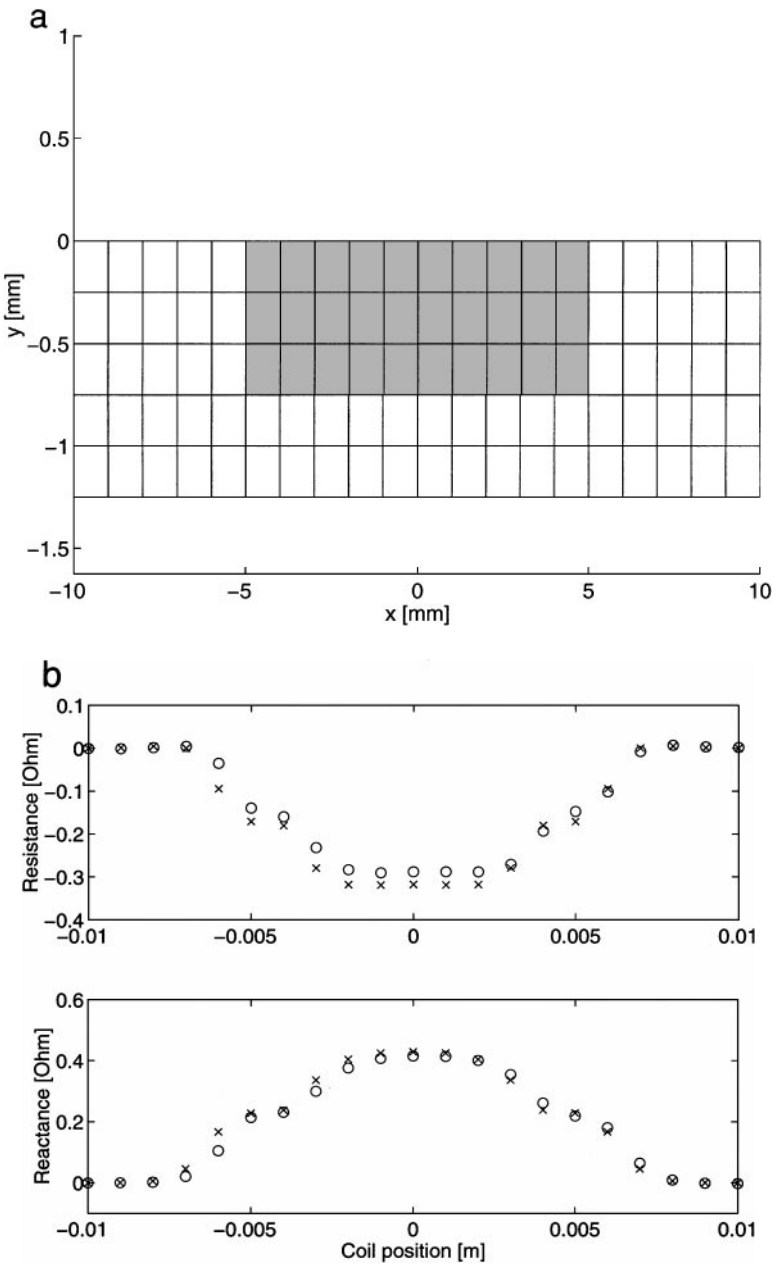

FIG. 3. Direct problem results: rectangular inner defect at 300 KHz. (a) Geometrical configuration; (b) impedance variation ($\circ =$ experimental values, $\times =$ simulated values).

on the basis of the figure of merit,

$$\varepsilon_F = \frac{\sqrt{\sum_n \left(R_n^{\text{guess}} - R_n^{\text{meas}}\right)^2}}{\sqrt{\sum_n \left(R_n^{\text{meas}}\right)^2}} + \frac{\sqrt{\sum_n \left(X_n^{\text{guess}} - X_n^{\text{meas}}\right)^2}}{\sqrt{\sum_n \left(X_n^{\text{meas}}\right)^2}},$$

where $R_n^{\text{meas}} + jX_n^{\text{meas}}$ (resp. $R_n^{\text{guess}} + jX_n^{\text{guess}}$) is the measured impedance variation (resp. the numerical impedance variation calculated for the current guess) at the nth position of

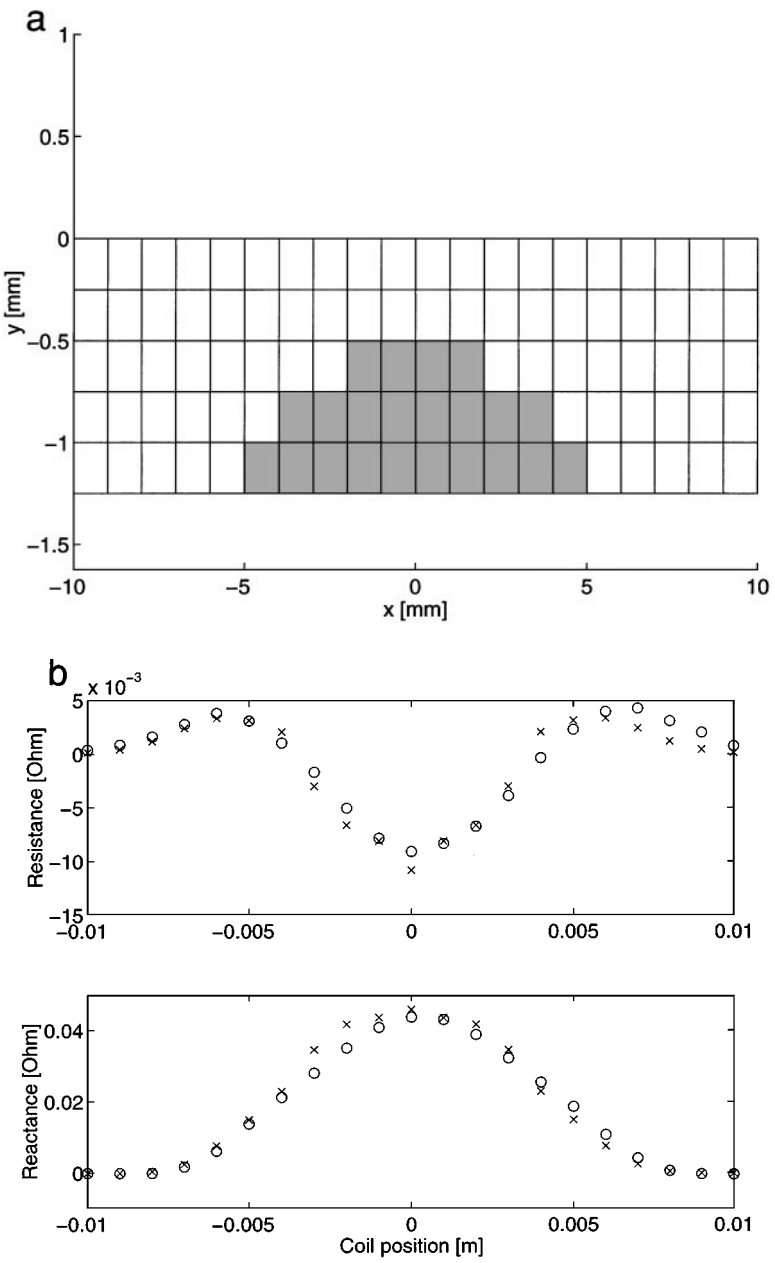

FIG. 4. Direct problem results: elliptical outer defect at 150 KHz. (a) Geometrical configuration; (b) impedance variation ($\circ$ = experimental values, $\times$ = simulated values).

the exciting coil. In Fig. 6 the results of the inversion procedure are presented in the case of the inner elliptical crack at 150 KHz.

In this figure, light gray stands for a facet which is in the crack both in reality and in the prediction, black indicates a facet which is not in the crack but is in the estimate, and dark gray stands for a facet which is in the real crack but not in the estimate. The results are clearly satisfactory: the bulk of the crack shape is correctly identified, with only a few bits wrong. In particular, the form of the crack illustrated in Fig. 6 is unsymmetric because the

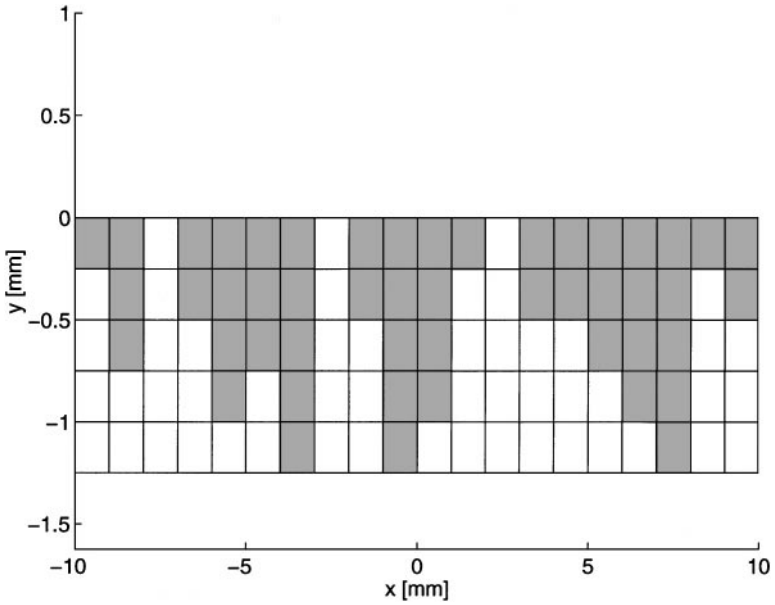

FIG. 5. Crack corresponding to the string [1 3 0 2 4 3 5 0 2 5 4 1 0 2 2 3 4 5 1 2].

measurements are not symmetric with respect to the $x = 0$ plane. In Table II some details are reported about the solution and the identification procedure, together with the value of the following shape error indicator,

$$\varepsilon_R = \frac{\text{area}(C_t \cup C_n - C_t \cap C_n)}{\text{area}(C_t)}$$

where C_t is the real crack and C_n is the identified crack.

Now we investigate the robustness of the method with respect to the problems related to ill-posedness, i.e., the effectiveness of our regularization strategy. In order to do this, we perform the inversion algorithm on data polluted by adding an artificial noise to the experimental data, which are already affected by experimental errors. If the regularization scheme is working properly the solution attained should be stable, i.e., to small variations of data there correspond small variations in the solution. In fact, this is the case, as one can see from the results shown in Fig. 7, where the errors ε_F and ε_R are plotted as functions of the standard deviation of the artificial noise.

Some comments are called for about the computational costs. The optimization algorithm used requires several solutions of the direct problem, each corresponding to a different

TABLE II
Information about the Inversion Algorithm

No. of generations	Time [s]	ε_R	ε_F
32	132	14.06%	18.65%

Note. The procedure run on a Pentium-based PC and stopped after 10 generations without any improvement of the error.

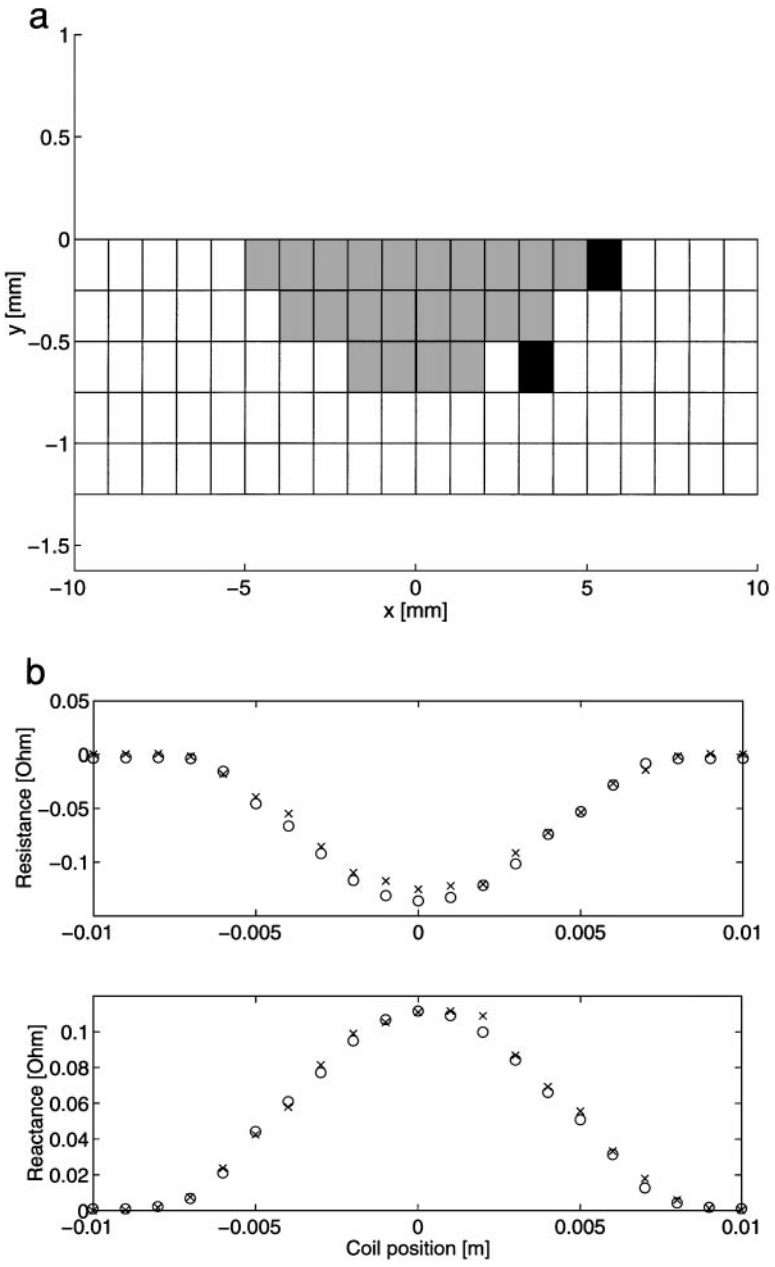

FIG. 6. Identification results for the inner elliptical crack at 150 KHz. (a) Geometrical configuration; (b) impedance variation ($\circ$ = experimental values, $\times$ = simulated values).

individual in the population. Since the $\mathbf{Z}'_{GG}$ matrix is computed once and for all, the only thing that must be done for a direct computation is only the inversion of a suitable submatrix. As mentioned before, at each step of the minimization procedure the dimension of the matrix to be inverted is at most $n_{\max} = n_T/2$. In the present case, it results in $n_{\max} = 50$; consequently, each subsequent direct calculation is extremely fast, which allows a very efficient implementation of genetic-like optimization strategies.

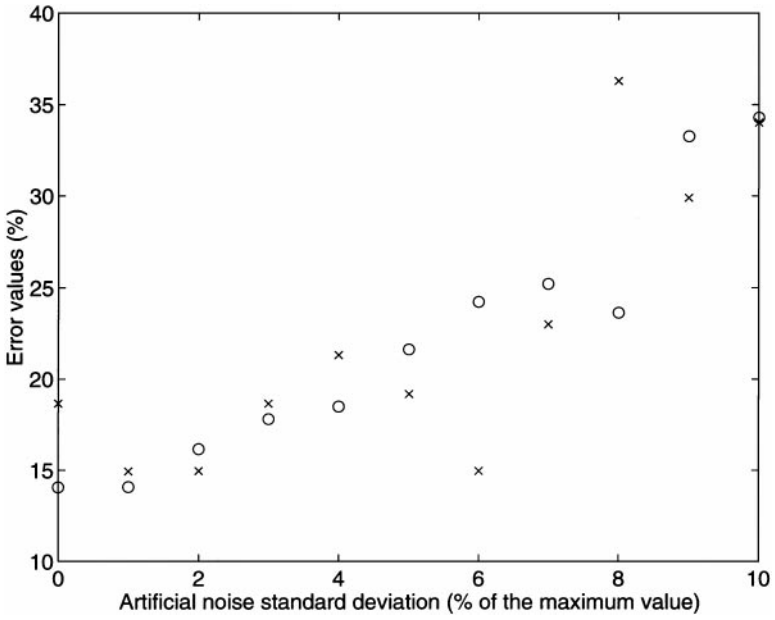

FIG. 7. Error values ε_F ($\circ$) and ε_R ($\times$) as a function of the standard deviation of the artificial noise (expressed in % of the maximum value of the measure).

VI. COMMENTS AND CONCLUSIONS

The numerical approach described here introduces a new efficient way to deal with the reconstruction of thin cracks. It is worth noticing that the technique introduced in this paper could be used also when dealing with volume cracks [24].

The method is based on an integral formulation which takes advantage of the edge element representation of the current density unknowns.

Its main characteristics can be better understood in comparison with other numerical approaches. Indeed, the present method combines the advantages of the integral formulations (the need of discretizing only the conducting region around the defect) with the differential finite element formulations where the knowledge of the analytic expression of the Green's function is not required. Moreover, the particular treatment of the unknowns in conjunction with the edge elements and the tree–cotree gauge condition gives automatic account of the solenoidality constraint, hence reducing to two the number of scalar unknowns related to the three components of the current density. In this way, the method allows us to take into account irregular domains containing steps, edges, and corners without any particular ad hoc artifices. In addition, when dealing with canonical geometries, the knowledge of the analytic solution for the unperturbed case can be effectively taken into account.

The advantages of this approach are related to the solutions of both the direct and the inverse problems. In the first case, it has been shown how fast and accurately a solution can be obtained for a given set of facets describing the defect. In the inverse problem, one key point is related to the binary nature of the unknowns which gives the possibility of conveniently exploiting the features of the genetic algorithm. In this way, the global minimum can be sought, hence reducing the problems related to the possible presence of the local minima.

The present method has been successfully applied to a number of benchmark problems. The predictions are in good agreement with the experimental data, and both the direct and the inverse computations are very fast. Hence, the method has proved to be very effective in tackling ECT problems.

APPENDIX: WOODBURY'S ALGORITHM

As stated in Section IV, the problem is to solve (41), which demands the inversion of the square matrix $\mathbf{Z}'_{FF}$, of dimensions $n_T - n_B$. We will show in this appendix that we can reformulate the problem so that the inversion of a square matrix of dimensions n_B is required. Hence, once the choice of the tentative subset B of facets has been made, the most convenient calculation can be performed.

Equation (41) can be rewritten as

$$\mathbf{Z}'_{FF}\delta\mathbf{G}_F + \mathbf{Z}'_{FB}\delta\mathbf{G}_B = \mathbf{0} \tag{A1}$$

$$\mathbf{Z}'_{BF}\delta\mathbf{G}_F + \mathbf{Z}'_{BB}\delta\mathbf{G}_B = \mathbf{q}_B \tag{A2}$$

or, in compact notation

$$\mathbf{Z}'_{GG}\delta\mathbf{G} = \mathbf{q}, \tag{A3}$$

where the vector $\mathbf{q} = [\mathbf{0}; \mathbf{q}_B]$ must be chosen so that $\delta\mathbf{G}_B = -\mathbf{G}_{0B}$. From (A3) we have

$$\delta\mathbf{G} = (\mathbf{Z}'_{GG})^{-1}\mathbf{q} = \mathbf{Z}''_{GG}\mathbf{q}, \tag{A4}$$

and hence, taking the definition of $\mathbf{q}$ into account,

$$\delta\mathbf{G}_B = \mathbf{Z}''_{BB}\mathbf{q}_B \tag{A5}$$

so that we must choose

$$\mathbf{q}_B = -(\mathbf{Z}''_{BB})^{-1}\mathbf{G}_{0B}. \tag{A6}$$

Hence, first of all we obtain the inverse $\mathbf{Z}''_{GG} = (\mathbf{Z}'_{GG})^{-1}$ once, and then we invert only the submatrix $\mathbf{Z}''_{BB}$ of dimensions n_B to obtain $\mathbf{q}_B$ and then, from (A4), $\delta\mathbf{G}$.

ACKNOWLEDGMENTS

The authors thank Dr. Roberto Petrillo for his help in producing the results. This work was partially supported by the INCO-COPERNICUS Project PL 964037 of the European Commission and by the Italian MURST.

REFERENCES

1. T. Takagi, M. Uesaka, and K. Miya, Electromagnetic NDE research activities in JSAEM, in *Electromagnetic Nondestructive Evaluation*, edited by T. Takagi *et al.* (IOS Press, 1997), p. 9.
2. D. Colton and R. Kress, *Inverse Acoustic and Electromagnetic Scattering Theory* (Springer-Verlag, Berlin, 1992).

3. D. Colton and L. Paivarinta, The uniqueness of a solution to an inverse scattering problem for electromagnetic waves, *Arch. Rational Mech. Anal.* **119**, 59 (1992).
4. V. Isakov, Uniqueness and stability in multidimensional inverse problems, *Inverse Problems* **9**, 579 (1993).
5. M. Yamamoto, A mathematical aspect of inverse problems for non-stationary Maxwell's equations, *Int. J. Appl. Electromagn. Mech.* **8**, 77 (1997).
6. T. Takagi, M. Hashimoto, *et al.*, Benchmark models of eddy current testing for steam generator tube: Experiment and numerical analysis, *Int. J. Appl. Electromagn. Mater.* **5**, 149 (1994).
7. J. R. Bowler, S. A. Jenkins, L. D. Sabbagh, and H. A. Sabbagh, Eddy-current probe impedance due to a volumetric flaw, *J. Appl. Phys.* **70**(3), 1107 (1991).
8. J. R. Bowler, L. D. Sabbagh, and H. A. Sabbagh, A theoretical and computational model of eddy current probes incorporating volume integral and conjugate gradient methods, *IEEE Trans. Magn.* **25**(3), 2650 (1989).
9. V. Monebhurrun, D. Lesselier, and B. Duchène, Eddy current nondestructive evaluation of a 3-D bounded defect in a metal tube using volume integral methods and nonlinearized inversion schemes, in *Electromagnetic Nondestructive Evaluation, II*, edited by R. Albanese *et al.* (IOS Press, 1998), p. 261.
10. J. Pavo and K. Miya, Reconstruction of crack shape by optimization using eddy current field measurement, *IEEE Trans. Magn.* **30**(5), 3407 (1994).
11. J. R. Bowler, Eddy current calculations using half-space Green's functions, *J. Appl. Phys.* **61**(3), 833 (1987).
12. C. T. Tai, *Dyadic Green's Functions in Electromagnetic Theory* (Intext, Scranton, 1971).
13. Z. Badics, Y. Matsumoto, S. Kojima, Y. Usui, K. Aoki, F. Nakayasu, and A. Kurokawa, Rapid flaw reconstruction scheme for three-dimensional inverse problems in eddy current NDE, in *Electromagnetic Nondestructive Evaluation*, edited by T. Takagi *et al*. (IOS Press, 1997), p. 303.
14. Z. Badics, Y. Matsumoto, K. Aoki, F. Nakayasu, M. Uesaka, and K. Miya, An effective 3D finite element scheme for computing electromagnetic field distorsion due to defects in eddy current nondestructive evaluation, *IEEE Trans. Magn.* **32**(3), 737 (1996).
15. Z. Chen, K. Miya, and M. Kurokawa, Reconstruction of Crack shapes using a newly developed ECT probe, in *Electromagnetic Nondestructive Evaluation, II*, edited by R. Albanese *et al.* (IOS press, 1998), p. 225.
16. R. Pierri and A. Tamburrino, On the local minima problem in conductivity imaging via a quadratic approach, *Inverse Problems* **13**, 1547 (1997).
17. R. Pierri, G. Rubinacci, A. Tamburrino, S. Ventre, and F. Villone, Nonlinear inverse resistivity profiling using wavelets, *IEEE Trans. Magn.* **34**(5), 2920 (1998).
18. G. Rubinacci, A. Tamburrino, and S. Ventre, A differential formulation based on a perturbative approach to solve the ECT inverse problem, *Comput. Methods Appl. Mech. Eng.* **169**, 407 (1999).
19. S. Norton and J. Bowler, Theory of ECT inversion, *J. Appl. Phys.* **73**(2), 501 (1993).
20. R. Albanese and G. Rubinacci, Integral formulation for 3-D eddy-current computation using edge elements, *IEE Proc.* **135**, 457 (1988).
21. R. Albanese and G. Rubinacci, Finite element methods for the solution of 3D eddy current problems, in *Advances in Imaging and Electron Physics* (Academic Press, San Diego, 1998).
22. C. J. Carpenter, Comparison of alternative formulations of 3-D magnetic field and eddy current problems at power frequencies, *IEE Proc.* **124**, 1026 (1977).
23. C. V. Dodd and W. E. Deeds, Analytical solutions to eddy-current probe-coil problems, *J. Appl. Phys.* **39**(6), 2829 (1968).
24. R. Albanese, G. Rubinacci, A. Tamburrino, and F. Villone, Reconstruction of cracks with integral methods, in *Electromagnetic Nondestructive Evaluation, II*, edited by R. Albanese *et al.* (IOS press, 1998), p. 107.
25. J. R. Bowler, Review of eddy current inversion with application to nondestructive evaluation, *Int. J. Appl. Electromagn. Mech.* **8**, 3 (1997).
26. H. Fukutomi, T. Takagi, J. Tani, and F. Kojima, Crack shape characterization in eddy current testing, in *Electromagnetic Nondestructive Evaluation, II*, edited by R. Albanese *et al.* (IOS Press, 1998), p. 305.
27. A. S. Householder, *The Theory of Matrix in Numerical Analysis* (Dover, New York, 1975).
28. J. A. Scales, M. L. Smith, and T. L. Fischer, Global optimization methods for multimodal inverse problems, *J. Comput. Phys.* **103**, 258 (1992).